

# Innovative approaches to waste heat recovery: Coupling high temperature vapour compression heat pumps with salt hydrate thermochemical systems<sup>☆</sup>

K. Malleswararao <sup>a,\*</sup>, Inga Bürger <sup>a</sup>, Aldo Cosquillo Mejia <sup>a</sup>, Seon Tae Kim <sup>b</sup>, Marc Linder <sup>a</sup>

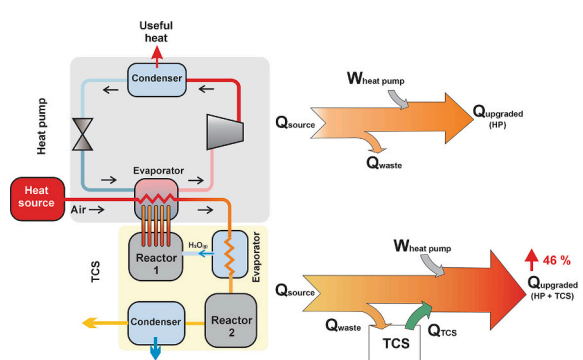
<sup>a</sup> Institute of Engineering Thermodynamics, German Aerospace Center (DLR), Pfaffenwaldring 38-40, Stuttgart, 70569, Germany

<sup>b</sup> Institute of Low-Carbon Industrial Processes, German Aerospace Center (DLR), Weinbergstraße 10, Cottbus 03050, Germany

## HIGHLIGHTS

- A novel dual-reactor TCES system configuration for waste heat recovery.
- Utilization of HTHP waste heat to simultaneously drive the charging and discharging of the TCES system.
- Emphasis on the design and operation of the evaporator and condenser within the TCES system.
- Thermodynamic analysis conducted to assess the performance of the proposed concept.
- With  $K_2CO_3$ , the system delivers 55.36 kW per kg/s of air at 140 °C with an efficiency of 45.68 %.

## GRAPHICAL ABSTRACT



## ARTICLE INFO

**Keywords:**  
 High temperature vapour compression heat pump  
 Advanced waste heat recovery  
 Thermochemical heat pump  
 Design aspects  
 Potassium carbonate

## ABSTRACT

Efficient utilization of waste heat is a crucial method to meet global energy demands and carbon neutrality. High Temperature mechanical Heat Pumps (HTHPs) are vital in this context but are limited by evaporator temperature constraints. This study proposes an innovative approach to upgrading and reintegrating waste heat from HTHPs (105–140 °C) by coupling them with a dual reactor salt hydrate based Thermo-Chemical Energy Storage (TCES) system. Operating in a quasi-continuous mode, the system utilizes the waste heat from the HTHP to drive hydration (discharge) in one reactor and dehydration (charge) in another. The key to heat upgrading lies in the evaporator of the TCES system, which governs system performance. Therefore, an empirical relation has been developed to determine its optimum temperature as a function of waste heat temperature, heat upgrade temperature, and the thermal properties of the salt hydrate. Subsequently, the system performance with  $K_2CO_3\text{-H}_2O$  was assessed by applying the first law of thermodynamics, with the evaporator temperature of the TCES varied from 100 °C to 90 °C. Lowering the evaporator temperature of the TCES enhances thermal output but is constrained by the HTHP's temperature requirements. The system delivers 55.4 kW per kg/s of air with a heat upgrade efficiency of 45.7 %, using waste heat at 140 °C and the evaporator of the TCES at 100 °C. This study attempts to establish a framework for designing efficient thermally driven cascaded heat pumps.

<sup>☆</sup> This article is part of a Special issue entitled: 'ICAE 2024(Y.Y)' published in Applied Energy.

\* Corresponding author.

E-mail address: [malleswararao.katamala@dlr.de](mailto:malleswararao.katamala@dlr.de) (K. Malleswararao).

Nomenclature		Subscripts
$A, B, C$	Constants of Antoine equation	$a$ Ambient/dry air
$c_p$	Specific heat capacity (J/kg.K)	$c$ Condenser
$h$	Enthalpy (J/kg)	$dh$ Dehydration
$\dot{m}$	Mass flow rate (kg/s)	$E$ Evaporator
$n$	Stoichiometric coefficient	$h$ Hydration
$p$	Pressure (bar or kPa)	$i$ Initial state
$\dot{Q}$	Heat transfer rate (W)	$in$ Inlet
$\tilde{R}$	Universal gas constant (J/mol.K)	$out$ Outlet
$T$	Temperature (K or °C)	$R$ Reactor
$W$	Compressor work (J)	$sl$ Switching losses
<i>Greek letters</i>		$w$ Water
$\Delta H_r^0$	Enthalpy of reaction (J/mol)	$wv$ Water vapour
$\Delta H_e$	Latent heat of evaporation (J/kg)	
$\Delta H_c$	Latent heat of condensation (J/kg)	
$\Delta S_r^0$	Entropy of reaction (J/mol.K)	
$\eta$	Efficiency (%)	
		Abbreviations
		COP Coefficient of performance
		HTF Heat transfer fluid
		HTHP High temperature heat pump
		TCES Thermochemical energy storage

## 1. Introduction

Efficient energy systems are desirable for addressing the rising energy demands while also attaining carbon neutrality. High Temperature Heat Pumps (HTHPs) based on vapour compression have been identified as a potential solution to this challenge, owing to their heat upgrade capabilities, energy efficiency, and environmental compatibility [1]. HTHPs upgrade the temperature of heat using external electrical work input to a mechanical compressor. Typical HTHPs operate between two pressure levels: the evaporator and condenser pressures, with the help of compression work. They function utilizing the phase-changing properties of a working fluid. There are numerous efforts that have been made to integrate HTHP technologies into existing industrial processes, considering both material and mechanical aspects. Several studies on HTHPs, including hybrid systems operating across different temperature levels, have demonstrated their industrial use [2,3]. However, their deployment in industrial applications is currently limited by the fact that most commercially available heat pumps are only capable of delivering heat at temperatures around 160–200 °C [4].

A key area of research focuses on extending the operational temperature range of HTHPs to broaden their applicability. While increasing the heat sink temperature can be achieved through the addition of multiple compression stages, expanding the lower limit of the heat source temperature range remains a fundamental challenge. This also pertains to their operational constraint that HTHPs require heat at a temperature higher than that of their evaporators, leaving waste heat below this threshold unused. This represents a significant opportunity for thermal energy recovery. This waste heat can be utilized in downstream processes that require lower temperatures than the preceding stages. Indeed, the effective recovery of low-temperature waste heat is crucial for improving the overall heat utilization efficiency of industrial processes. Another critical challenge to consider is the increased temperature difference between the heat source and the heat sink. While recovering low-temperature heat can enhance the overall utilization efficiency of industrial processes, a larger temperature difference can result in a lower Coefficient of Performance (COP). The COP, which serves as a measure of a heat pump's efficiency, quantifies the amount of heat delivered to the heat sink (condenser) per unit work input to the compressor. According to the Carnot cycle, achieving a higher temperature lift requires higher pressures, which demand greater compression work, thus increasing the mechanical/electrical energy input required to achieve the desired temperature rise. As a result, the trade-off between temperature lift and efficiency becomes more pronounced, as higher

compression work reduces the overall COP of the system. In this regard, if the waste heat of the HTHP is collected, upgraded, and reintegrated into the process at higher temperatures without using additional electrical/mechanical energy (i.e., without employing another low-temperature mechanical HP), it would further enhance the energy efficiency and sustainability of the system. Since heat supply at higher temperatures increases both the evaporation rate and the pressure of the working fluid, the workload of the compressor is reduced, requiring less mechanical energy to compress the vapour to the desired conditions. Consequently, the overall efficiency of the HTHP improves, leading to more energy-efficient operation.

Pertaining to the above context, Thermo-Chemical Energy Storage (TCES) systems, which rely on low-grade energy, offer significant potential for thermal energy storage and heat pump applications. A key advantage of TCES is the dependence of reaction temperature on gas pressure, which allows for thermal energy upgrading. Higher gas pressures result in elevated hydration reaction temperatures, distinguishing TCES from sensible and latent heat storage systems. Several experimental studies have shown the viability and effective performance of these systems [5–8]. Thus, integrating HTHPs with TCES systems to capture and upgrade their low-temperature waste heat would be essential for enhancing HTHPs performance and efficiency.

Motivated by this objective, the authors previously proposed several potential configurations for a novel quasi-continuously operated dual-reactor TCES system based on salt hydrates, aimed at recovering waste heat from HTHPs and integrating upgraded heat into their processes [9]. In that work, the optimum configuration was identified, and a screening methodology was established for selecting suitable salt hydrates. This novel concept advances the idea of incorporating a salt hydrate reactor for thermal energy storage and heat upgrading within existing HTHP systems, as presented by Richter et al. [10] and Kim et al. [11], while providing operational strategies and design considerations for quasi-continuous waste heat recovery. Building on this foundation, the present study emphasizes the critical role of the evaporator and its design in TCES systems, which has not been extensively addressed in the literature. Furthermore, it discusses the benefits and limitations of incorporating a condenser into the salt hydrate system for water vapour recovery during the dehydration process.

Salt hydrates materials are known for their cost-effectiveness, energy storage density, safety, and ease of maintenance due to their operation with water vapour at low pressures as reported by Chen et al. [12] and Bouché et al. [13]. During charging, waste heat is collected through an endothermic reaction as salt hydrate decomposes into salt and water

vapour. The reverse exothermic reaction releases stored heat during salt hydrate formation. For a solid-gas reaction based TCES systems, the van't Hoff eq. [14] demonstrates the relationship between the pressure,  $p_{eq}$  (kPa), of gas and the temperature,  $T_r$  (K), of the porous bed in equilibrium. It is expressed as,

$$\ln\left(\frac{p_{eq}}{p_0}\right) = \frac{\Delta S_r^o}{R} - \frac{\Delta H_r^o}{RT_r} \quad (1)$$

Here,  $\Delta H_r^o$  (kJ/mol) and  $\Delta S_r^o$  (kJ/(mol.K)) represent the changes in standard enthalpy and entropy during the salt-water vapour interactions, respectively.  $R$  (J/(mol.K)) is the universal gas constant, and  $p_0$  is the reference pressure, typically 1 bar. From Eq. (1), it is evident that supplying water vapour to the salt bed at higher pressures increases reaction temperatures, acting as a thermochemical heat pump. This insight is key for designing evaporators and condensers to achieve target heat delivery temperatures and optimize waste heat utilization.

Several studies have highlighted the significant potential of salt hydrate-based heat pumps and heat transformers. Richter et al. [10] explored a thermochemical heat transformer utilizing  $\text{CaCl}_2$  in a closed-loop system, achieving a 35 K temperature increase with charging at 130 °C. In a separate study, their group demonstrated that the system could achieve temperature upgrades of up to 65 K using direct heat transfer methods [13]. Recently, Michel et al. [15] reported a temperature rise exceeding 60 K at a specific power of 341 W/kg using a salt deposit configuration. Similarly, Esaki et al. [16] showed that a thermochemical heat pump could upgrade heat from 100 °C to 155 °C, with the condenser and evaporator operating at 25 °C and 97 °C, respectively, achieving a volumetric heat transfer rate of 322 kW/m<sup>3</sup>. A recent thermodynamic and techno-economic evaluation by Kim et al. [11] highlights the potential of integrating a HTHP with thermal energy storage for waste heat recovery. Two TES systems integrated with a HTHP, were analyzed: sensible heat storage using concrete and TCES using  $\text{SrBr}_2/\text{H}_2\text{O}$ . The TCES system showed significantly higher efficiency and temperature output (196–228 °C). Over 20 years, the HTHP-TCES system achieved a net present value of up to € 464,559, demonstrating strong potential for improving industrial energy efficiency. These results demonstrate the role of TCES systems in enhancing energy efficiency in industrial processes.

To fully exploit the potential of salt hydrates for heat pumping, it is critical to select suitable operating temperatures and corresponding salt hydrate materials for optimal use of heat sources in cascaded HTHP-TCES systems. Notably, around one-third of industrial waste heat in the European Union [16] and 42 % globally [17] is available at temperature levels below 200 °C, highlighting the importance of utilizing this heat to reduce fossil fuel dependence and promote carbon-neutral energy systems. In this context, the present research investigates possibilities to recover waste heat from HTHPs using a quasi-continuous TCES system operating at 105–140 °C, upgrading the heat and returning it to the HTHP at higher temperatures.

Subsequently, drawing from existing research [9,19,20], Potassium carbonate ( $\text{K}_2\text{CO}_3$ ) has been identified as a suitable material due to its compatibility with the target operating conditions and favorable thermal properties. The selection criteria included temperature/pressure range, energy density, cyclic stability, and chemical compatibility, based on a screening method developed by the authors in their previous work [9]. The authors also established a correlation between air inlet and outlet temperatures and water vapour content, analyzing with a reference material  $\text{K}_2\text{CO}_3$ , which provides fundamental insights for the efficient thermal design of a salt hydrate reactor with direct heat transfer using air as the Heat Transfer Fluid (HTF) as well as the mass source/sink. Studies by Sögütoglu et al. [19] and Houben et al. [21] confirmed the cyclic stability of  $\text{K}_2\text{CO}_3$ , with the latter highlighting its suitability for direct charging, where hot air as HTF flows through the bed to optimize temperature use. Donkers et al. [22] reported an energy storage density of 1.3 GJ/m<sup>3</sup> on material level. Recent studies by Salehzadeh

et al. [23] and Elahi et al. [24] demonstrated that encapsulated porous  $\text{K}_2\text{CO}_3$  granules enhance both cyclic stability and diffusion kinetics, making them promising for TCES applications.

Based on the preceding discussion, this study presents the essential features of the proposed novel configuration for the cascaded TCES-HTHP system. The key components of the TCES subsystem, which significantly impact the overall system performance, are then discussed. Since the heat output temperature of TCES is determined by its vapour pressure, i.e., its evaporator, special emphasis is placed on its design and operation. Subsequently, a correlation is developed to determine its optimal operating temperature as a function of the waste heat temperature, the hydration reaction temperature, and the thermal properties of the salt hydrate. Finally, a thermodynamic analysis is performed on the TCES subsystem to evaluate the effects of both the evaporator and waste heat temperatures on system performance.

## 2. Configuration of a novel cascaded TCES-HTHP system

In general, a conventional cascaded HP system consists of an HTHP integrated with a low temperature HP with a different working fluid in each HP. This cascaded HP requires electric/mechanical work input for temperature uplifting which is energy expensive. The objective of the present study is to upgrade the waste heat to useful heat without using high grade energy. In this regard, the present study proposes a thermally driven cascaded TCES-HTHP system with air as the HTF, as shown in Fig. 1. Exit air of the HTHP supplies waste heat to the evaporator to generate water vapour that is subsequently utilized to discharge heat from Reactor 1 at the required temperature ( $T_{dc} > T_s$ ), and subsequently goes on to charging Reactor 2, followed by passage through a condenser to recover water vapour. Here, Reactor 1 is operated through indirect heat transfer (discharging) and Reactor 2 is operated through direct heat transfer (charging). Under the limiting case for design criteria, the air passing directly through the salt hydrate bed in Reactor 2 exits fully saturated. This temperature is the lowest attainable by the process, but it must be higher than the ambient temperature at which Reactor 2 is intended to operate. The characteristics of direct and indirect heat transfer as well as the possible configurations of the proposed concept of cascaded HPs were discussed qualitatively in a recent study by the authors [9]. TCES systems utilizing direct heat transfer are reported to offer superior heat transfer efficiency due to reduced thermal resistance, and have been shown to be cost-effective and high-performing in previous research [25,26]. Operating pressure-less, as air circulates in an open loop, enables the condenser to function at ambient conditions. When Reactor 1 completely discharges heat, i.e., becomes saturated with water vapour, the functions of Reactor 1 and Reactor 2 are switched during the second half of the cycle. So that Reactor 2 then takes over the discharging role, while Reactor 1 switches to charging. This arrangement allows the system to operate in a quasi-continuous cycle.

The proposed configuration, shown in Fig. 1, presents a promising solution for the intended application. Supplying pure water vapour at absolute pressure to Reactor 1 ensures elevated hydration temperatures and the heat pipes facilitate effective isothermal heat transfer. Simultaneously, the direct passage of dry air through Reactor 2 enables better use of air for the charging process. With direct contact and operation close to atmospheric pressure, this configuration simplifies the reactor design and enhances operational efficiency.

The described concept could offer a heat pump effect without the need for absolute pressure swings, providing a significant advantage compared to conventional pressurized or evacuated systems. This close-to-atmospheric operation simplifies system design, reduces mechanical complexity, and minimizes risks associated with vacuum maintenance or high-pressure vessels. However, a major potential drawback lies in the continuous loss of water during operation. Even with the use of a condenser, which must be operated at ambient temperature to avoid additional electricity consumption that would undermine the effectiveness of low-temperature waste heat recovery, only a fraction of the

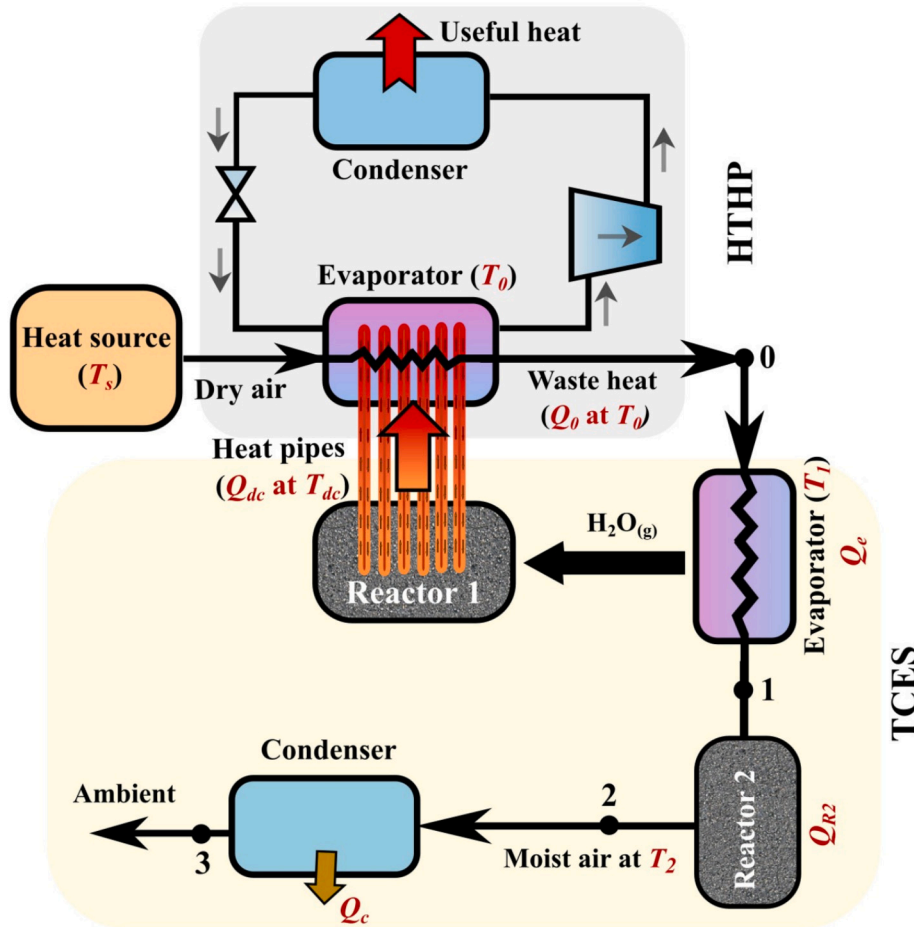


Fig. 1. Configuration of the cascaded TCES-HTHP system.

water can be recovered. This limitation was highlighted by the authors in their previous study [9].

An analogy to this concept could be drawn from spray cooling of ambient air with the evaporation of fine water droplets. In such systems, the thermal effect achieved is inherently tied to a continuous consumption of water. An obvious first step toward addressing this limitation could involve the use of wastewater streams as the evaporator input. Utilizing industrial or municipal wastewater offers a dual benefit: reducing freshwater demand and contributing to water reuse objectives. However, the use of wastewater may introduce challenges such as fouling, salt scaling, or contamination of instrumentation, depending on the composition of wastewater.

By shifting the perspective, the quasi-continuous salt hydrate system presents an opportunity for synergistic integration with conventional thermal desalination methods using low-temperature waste heat. In the proposed system, shown in Fig. 1, seawater can be evaporated using waste heat in the evaporator, releasing useful heat through an exothermic reaction in Reactor 1. The seawater is then condensed back into freshwater during dehydration in Reactor 2. When combined with low-grade industrial waste heat, this approach could improve the efficiency of freshwater production from seawater. Ng et al. [27] and Mitra et al. [28] investigated adsorption desalination systems based on silica gel-water using low-temperature heat at 85 °C, demonstrating the operational viability of the concept.

It may be noticed that the condenser located after Reactor 2 is designed to capture water vapour from the moist air collected from the salt hydrate bed during the charging process by operating at ambient temperature, thus avoiding additional operational costs. In this context, it is essential that the ambient temperature remains low enough to

ensure that the saturation pressure of the condenser is lower than the vapour pressure of water in the air exiting Reactor 2. Depending on the scale of the system, if the benefits associated with condensing the water vapour from the moist air exiting Reactor 2 are outweighed by the costs associated with operating the condenser, it may be more efficient to omit the condenser altogether and discharge the air directly into the ambient environment. This would also reduce the complexity of the system and improve operational efficiency, though it may entail a degree of water vapour loss to the surrounding environment.

The thermodynamics of the proposed cascaded HP system can be explained using a van't Hoff plot, as shown in Fig. 2. The plot illustrates that the HTHP operates at temperatures above  $T_0$ , while thermal energy below  $T_0$  can be effectively utilized with the TCES system. As depicted in Fig. 2, air enters the evaporator of the TCES system at  $T_0$ , and it supplies heat to the evaporator until it reaches  $T_1$ , facilitating the generation of water vapour. This water vapour is then directed to Reactor 1, where it induces an exothermic reaction with the salt releasing the heat at a temperature corresponding to its equilibrium temperature. Subsequently this heat is transferred to the HTHP. The air, then at  $T_1$ , flows into Reactor 2 for charging, where its temperature decreases further to  $T_2$ . Simultaneously, its humidity increases as it absorbs water vapour released from Reactor 2 due to the endothermic reaction. The air then passes through a condenser, where the water vapour is recovered. Subsequently, Reactor 1 and Reactor 2 are switched, thereby transitioning the system to a quasi-continuous mode of operation.

In summary, the proposed cascaded heat pump system exploits thermal energy below  $T_0$  in two distinct ways: First, the thermal energy between  $T_0$  and  $T_1$  is harnessed to evaporate water, thereby discharging one reactor at  $T_{dc}$ , thus achieving a heat pump effect. Second, the

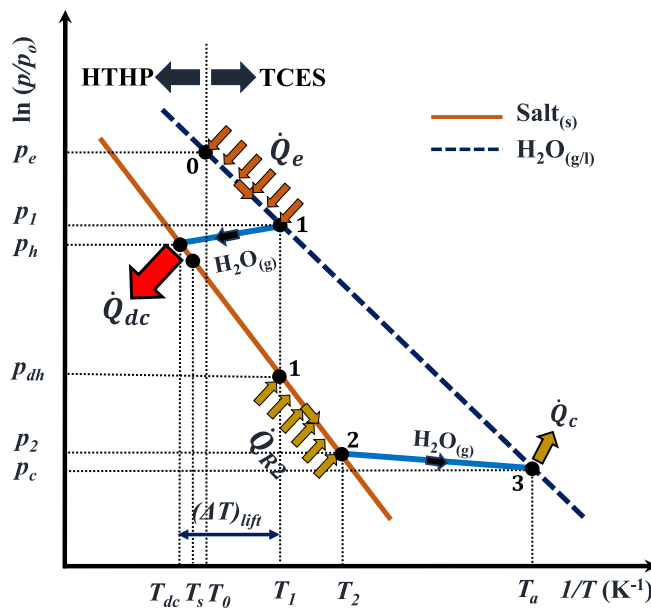


Fig. 2. van't Hoff plot for the ideal operation of the cascaded system.

thermal energy between  $T_1$  and  $T_2$  is utilized to charge the second reactor via direct heat transfer.

### 3. Significance of the evaporator in TCES system

It is well-known that TCES systems are pressure-driven reaction temperature systems [19]. It implies that the temperature of solid-gas reactions is governed by the pressure of the gas/water vapour. In the proposed cascaded TCES-HTHP system (Fig. 1), the evaporator of TCES utilizes the waste heat from HTHP at  $T_0$  to supply water vapour to Reactor 1 at the required pressure, thereby achieving the desired heat discharge temperature ( $T_{dc}$ ). This temperature,  $T_{dc}$ , must be higher than the waste heat temperature ( $T_0$ ) to produce the useful output of the proposed concept. The pressure of the evaporator is determined by its operating temperature ( $T_1$ ). Therefore, the evaporator is a core component of the TCES, and its operating temperature plays a crucial role in achieving the desired heat delivery temperature (heat pumping effect,  $\Delta T_{lift}$ ). In this regard, it is essential to determine the required minimum temperature of the evaporator to achieve the intended heat discharge temperature which must be higher than the waste heat temperature of the HTHP. Ideally, with an efficient heat transfer mechanism, the heat discharge temperature ( $T_{dc}$ ) of Reactor 1 should closely align with its reaction temperature ( $T_r$ ), corresponding to the equilibrium pressure ( $p_{eq}$ ) of water vapour. Consequently, in the following section, a mathematical constraint to determine the required evaporator temperature has been formulated as a function of the waste heat temperature of the HTHP, the required heat delivery temperature and the thermal properties of the salt hydrate material.

Recalling Eq. (1) that provides a relationship between the equilibrium pressure and temperature of a salt hydrate system,

$$\ln\left(\frac{p_{eq}}{p_0}\right) = \frac{\Delta S_r^o}{R} - \frac{\Delta H_r^o}{R T_r}$$

$$\Rightarrow T_r = \frac{\Delta H_r^o}{\Delta S_r^o - \tilde{R} \ln\left(\frac{p_{eq}}{p_0}\right)} \quad (2)$$

Based on Eq. (2),  $T_r$  would fall below a negative value if  $\Delta S_r^o - \tilde{R} \ln\left(\frac{p_{eq}}{p_0}\right) < 0$ , a situation that is practically infeasible.  $T_r$  will be maximum when the equilibrium pressure of the salt hydrate bed ( $p_{eq}$ ) is

maximum if  $\Delta S_r^o - \tilde{R} \ln\left(\frac{p_{eq}}{p_0}\right) > 0$ . The maximum value of  $p_{eq}$  that it can attain during hydration in an ideal case is when it equals the supply pressure of water vapour, i.e., the evaporator pressure  $p_e$ . Therefore,  $T_r$  is maximum when  $p_{eq} \approx p_e$ . For this purpose, it is essential to ensure the availability of an infinite source of water vapour whose pressure is unaffected by the reactor pressure when both are coupled. Consequently, the equilibrium pressure of the salt hydrate corresponds to the pressure within the evaporator. As a result, Eq. (2) can be expressed as follows:

$$T_r = \frac{\Delta H_r^o}{\Delta S_r^o - \tilde{R} \ln\left(\frac{p_e}{p_0}\right)} \quad (3)$$

The objective of the cascaded TCES-HTHP is that the temperature of heat delivery from the TCES should be higher than the waste heat temperature of the HTHP, i.e.,  $T_r > T_0$ , which can also be written based on Eq. (3) as,

$$\frac{\Delta H_r^o}{\Delta S_r^o - \tilde{R} \ln\left(\frac{p_e}{p_0}\right)} > T_0, \text{ if } \Delta S_r^o - \tilde{R} \ln\left(\frac{p_e}{p_0}\right) > 0 \quad (4)$$

The evaporator must supply water vapour to Reactor 1 for hydration reaction at a pressure corresponding to which the hydration temperature of the salt hydrate is higher than the waste heat temperature of the HTHP. Consequently, it is essential to determine the required temperature of the evaporator that results in the desired pressure of water vapour. The Antoine Eq. [29] offers an empirical formula that closely approximates the saturation pressure of water vapour at a given temperature, as shown below.

$$\log_{10} p_e = A - \frac{B}{C + T_e} \quad (5)$$

where,  $T_e$  in °C and  $p_e$  in mmHg. The constants A, B and C are all positive quantities; 8.07131, 1730.63 and 233.426 for temperatures in the range of 1 °C to 99 °C and 8.14019, 1810.94 and 244.485 in the range of 100 °C to 374 °C, respectively. The Antoine equation demonstrates an accuracy within ±1 % over the 0–100 °C range for water vapour pressure, with deviations of -0.93 % at 0 °C and +0.02 % at 100 °C, when compared to values from the Lide table [30], a widely accepted source of thermodynamic data. Within the evaporator's operating temperature range of 90–100 °C relevant to this study, the accuracy improves further to between -0.13 % and +0.02 %, representing negligible error. Correspondingly, the equilibrium reaction temperature for  $K_2CO_3$  estimated using vapour pressures calculated via the Antoine equation deviates by only -0.003 % to +0.02 %, an effect sufficiently small to be considered insignificant on system performance metrics. Consequently, no numerical smoothing of data was deemed necessary for the analysis. Eq. (5) can be re-written as,

$$p_e = 10^{A - \frac{B}{C + T_e}} \quad (6)$$

Placing Eq. (6) in Eq. (4) provides an expression for the required minimum evaporator temperature as a function of the waste heat source temperature and the thermal properties of the salt hydrate.

$$\frac{\Delta H_r^o}{\Delta S_r^o - \tilde{R} \ln\left(\frac{10^{A - \frac{B}{C + T_e}}}{p_0}\right)} > T_0, \text{ if } \Delta S_r^o - \tilde{R} \ln\left(\frac{10^{A - \frac{B}{C + T_e}}}{p_0}\right) > 0$$

$$\Rightarrow A - \frac{B}{C + T_e} > \log_{10} \left( p_0 \times e^{\frac{\Delta S_r^o - \Delta H_r^o}{R T_0}} \right)$$

$$\Rightarrow \begin{cases} T_e > \frac{B}{A - \log_{10} \left( p_0 \times e^{\frac{\Delta S_r^0}{R} - \frac{\Delta H_r^0}{RT_0}} \right)} - C, \text{ if } 0 < A - \log_{10} \left( p_0 \times e^{\frac{\Delta S_r^0}{R} - \frac{\Delta H_r^0}{RT_0}} \right) < 7.41 \\ T_e > 0 \text{ K, if } A - \log_{10} \left( p_0 \times e^{\frac{\Delta S_r^0}{R} - \frac{\Delta H_r^0}{RT_0}} \right) < 0 \end{cases} \quad (7)$$

Eq. (7) provides the mathematical expression for the required minimum evaporator temperature to achieve the intended heat pumping effect by the TCES system. Here, 7.41 is the ratio between the constants B and C of the Antoine equation (Eq. (5)). It is to be noticed that in Eq. (7),  $p_0$  should be in mmHg.

It is important to note that for TCES systems designed for heat upgrade applications, achieving substantially higher heat delivery temperatures than the heat sink is crucial to establish the necessary temperature gradients for efficient heat transfer. Here, the evaporator of the HTHP is the heat sink for the TCES system. Consequently, the evaporator of the TCES system needs to be operated at relatively higher temperatures than its minimum required temperature to ensure that it produces vapour at higher pressures. For instance, if the specified system operation requires the upgraded heat at a temperature 15 K higher than the evaporator temperature of the HTHP, the corresponding evaporator temperature of the TCES that results in the required heat discharging temperature of Reactor 1 can be determined by replacing ' $T_0$ ' with ' $T_0 + 15$ ' in Eq. (7). Indeed, the higher heat delivery temperatures indicate the higher quality of heat (higher availability). Fig. 3 shows the required minimum evaporator temperatures ( $T_e$ ) of TCES and the corresponding saturation pressures of water vapour that are necessary for achieving the hydration temperature ( $T_{de}$ ) 15 K higher than the waste heat temperature ( $T_0$ ) of the HTHP.

Fig. 3 presents an example calculation of the required evaporator temperature and its corresponding pressure for  $\text{K}_2\text{CO}_3$ , based on a specified waste heat temperature from an HTHP. Based on Fig. 3, it is observed that within the waste heat temperature range considered in the

present study, the minimum possible saturation vapour pressures required to reach the desired heat upgrade temperatures occur at vacuum pressures. Therefore, operation of reactors at atmospheric pressure is not feasible. Consequently, a specialized reactor design for salt hydrates would be necessary to accommodate the resulting pressure differential. However, it would be clearly advantageous if the salt hydrate reactors can operate at or near atmospheric pressure, as this allows for pressure-free operation, thereby reducing the need for specialized design and maintenance during experimentation. To achieve this, the evaporator must operate at temperatures close to 100 °C. This operational regime also enables higher hydration temperatures than rated, thereby enhancing the heat pumping effect as well as the efficiency of the HTHP. Operating the evaporator of TCES at relatively higher pressures, i.e., close to the atmospheric pressure, would also significantly enhance the efficiency of the HTHP. Because this facilitates the Reactor 1 to supply heat to the HTHP at significantly higher temperature than its evaporator temperature and thus contributes in thermal compression of the vapour. Consequently, it reduces the work required by the compressor of the HTHP to compress the vapour to the specified pressure of its condenser. It is important to note that Reactor 2 can consistently operate pressure-less, irrespective of the operating conditions in Reactor 1, as it operates with the direct flow of air at atmospheric pressure.

As stated earlier, the study aims to utilize the waste heat in the range of 105 °C to 140 °C ( $T_0$ ). Therefore, the TCES system must upgrade heat above  $T_0$ , requiring the evaporator to supply water vapour at a pressure that achieves significantly higher reaction temperatures ( $T_r$ ) in Reactor 1 than  $T_0$ . As a case study, the evaporator temperature ( $T_e$ ) is varied from 100 °C to 90 °C in steps of 5 °C to investigate its pressure effect on the

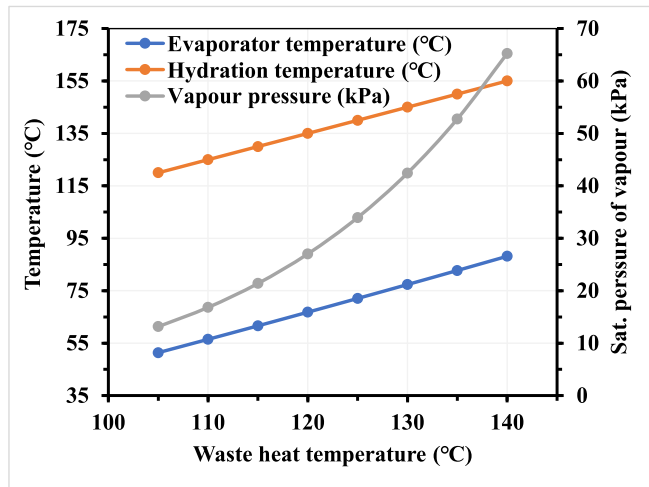


Fig. 3. Evaporator temperature and pressure required for  $\text{K}_2\text{CO}_3$  at various waste heat temperatures.

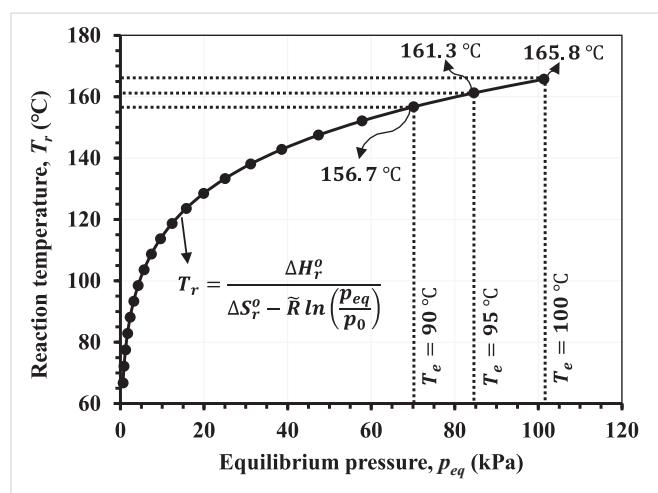


Fig. 4. Hydration temperature variation with equilibrium pressure of water vapour.

system performance while also ensuring the reaction temperature is more than the 140 °C which is the maximum waste heat temperature consider for the analysis.

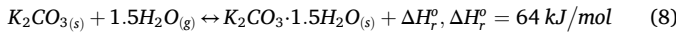
In the present study, the minimum evaporator temperature is constrained to 90 °C to ensure higher hydration temperatures, thereby maximizing the heat pumping effect, while also avoiding the operation of the reactor at excessively low vacuum pressures. The variation in the hydration temperature of K<sub>2</sub>CO<sub>3</sub> salt hydrate with the equilibrium pressure of water vapour is plotted as shown in Fig. 4. The saturated water vapour pressure at 100 °C, 95 °C and 90 °C is estimated as 101.325 kPa, 84.529 kPa and 70.117 kPa, respectively, and the corresponding equilibrium reaction temperature of K<sub>2</sub>CO<sub>3</sub>-water vapour system is 165.75 °C, 161.26 °C and 156.72 °C, respectively, estimated using van't Hoff equation Eq. (1). The evaporator temperature/pressure is chosen in such way that it results in significantly higher heat delivery temperatures than the maximum assumed waste heat temperature (140 °C) as shown in Fig. 4.

The effect of the TCES evaporator temperatures on the system overall performance is evaluated and discussed in the subsequent sections.

#### 4. Thermodynamic analysis of the TCES system

In this section, a thermodynamic analysis is performed to evaluate the performance of the proposed concept. The study investigates the effect of the temperatures of the waste heat source and the evaporator of TCES on system performance. The analysis focuses on the TCES with K<sub>2</sub>CO<sub>3</sub> bed in both reactors and the temperature of air at the inlet of the evaporator ( $T_0$ ) of TCES is varied from 105 °C to 140 °C. Given the existing literature on characterization of K<sub>2</sub>CO<sub>3</sub> salt hydrate [19–21,31], K<sub>2</sub>CO<sub>3</sub> has been chosen as the reference material for this study, based on its potential to operate within the specified temperature range. While its performance is anticipated, further experimental investigations are essential to validate its practical applicability and functionality, especially considering the metastable zone and deliquescence. Indeed, this analysis is applicable to any salt hydrate that operates within this temperature range and is suitable for direct heat and mass transfer with air without side reactions. The two reactors are assumed to contain enough quantity of K<sub>2</sub>CO<sub>3</sub> material to react with the water vapour fully and spontaneously. The TCES evaporator operates at 90–100 °C, and the air temperature at the evaporator exit is considered to be equal to the evaporator temperature. The condenser is operated at 20 °C.

The stoichiometric equation of K<sub>2</sub>CO<sub>3</sub>-H<sub>2</sub>O reaction [20] is given as the following,



Waste heat of HTHP:

The available waste heat from the HTHP supplied to the TCES using air as an HTF can be quantified as,

$$\dot{Q}_{HTP} = \dot{m}_a \times c_{p,a} \times (T_0 - T_a) \quad (9)$$

where,  $\dot{m}_a$  (kg/s) and  $c_{p,a}$  (kJ/(kg.K)) are the air mass flow rate and specific heat capacity, respectively.

**Evaporator of TCES:** The heat supplied to the evaporator and the resulting rate of vapour generation are estimated as follows.

Heat supplied by the air stream,

$$\dot{Q}_a = \dot{m}_a \times c_{p,a} \times (T_0 - T_1) \quad (10)$$

Heat received by the evaporator,

$$\dot{Q}_E = \dot{m}_{wv} \times (\Delta H_e + c_{p,w} \times (T_1 - T_a)) \quad (11)$$

where,  $\Delta H_e$  (kJ/kg) is the latent heat of evaporation at the specified evaporator operating temperature. Eq. (11) also considers the sensible heat required for the water vapour to reach its evaporation temperature from ambient temperature. The eqs. (10) and (11) are equal due to

energy balance across the evaporator. Consequently, the rate of water vapour generation can be estimated as,

$$\dot{m}_{wv} = \frac{\dot{m}_a \times c_{p,a} \times (T_0 - T_1)}{\Delta H_e + c_{p,w} \times (T_1 - T_a)} \quad (12)$$

**Reactor 1 of TCES:** Reactor 1 essentially acts as a thermochemical heat pump. It delivers heat at the required temperatures of the HTHP and it is estimated using the rate of water vapour it receives from the evaporator and the standard enthalpy of reaction of K<sub>2</sub>CO<sub>3</sub> as,

$$\dot{Q}_{R1} = \dot{m}_{wv} \times \Delta H_r^0 \quad (13)$$

**Reactor 2 of TCES:** The thermal energy of air stream after the evaporator of TCES system is harnessed to charge Reactor 2. Simultaneously, as it passes through the salt hydrate bed in Reactor 2, the air stream captures water vapour released from it due to the endothermic reaction. Heat supplied to Reactor 2 is estimated as,

$$\dot{Q}_{R2} = \dot{m}_a \times (h_{in,R2} - h_{out,R2}) = \dot{m}_{wv} \times (\Delta H_r^0 + c_{p,wv} \times (T_1 - T_2)) \quad (14)$$

where  $h_{in,R2}$  and  $h_{out,R2}$  are the enthalpies (kJ/kg) of air at the inlet and outlet of Reactor 2, respectively. The enthalpy of moist air at the outlet of Reactor 2 is the total enthalpies of dry air and water vapour ( $h = h_a + \omega h_{wv}$ ). Here,  $\omega$  (kg of water vapour per kg of dry air) is the specific humidity for air. The enthalpy of dry air can be estimated approximating it as an ideal gas as,

$$h_a = c_{p,a}T, (T \text{ in } ^\circ\text{C}).$$

The enthalpy of water vapour can be written as [32],

$$h_{wv} \cong 2501 + 1.82T, (T \text{ in } ^\circ\text{C}).$$

Operational constraint:

A crucial constraint considered in this study to ensure consistency in quasi-continuous operation of reactors is, the rate of water vapour supplied to Reactor 1 equals the rate of water vapour released by Reactor 2. The temperature of air at the outlet of Reactor 2 is then derived using Eqs. (12) and (14):

$$T_2 = \frac{(c_{p,a}T_1 - 2501\omega_2)[\Delta H_e + c_{p,w}(T_1 - T_a)] + c_{p,a}(T_0 - T_1)[c_{p,wv}T_a - \Delta H_r^0]}{c_{p,a}c_{p,wv}(T_0 - T_1) + (c_{p,a} + 1.82\omega_2)[\Delta H_e + c_{p,w}(T_1 - T_a)]} \quad (15)$$

here, the specific humidity of outlet air is estimated using the principles of psychrometry [18,32]. Considering that the water vapour fraction in the moist air is minimal compared to the dry air, the constraint of equal water vapour masses of Reactor 1 and 2 results in the following equation:

$$\frac{T_0 - T_1}{T_1 - T_2} = \frac{\Delta H_e + c_{p,w} \times (T_1 - T_a)}{\Delta H_r^0 + c_{p,wv} \times (T_1 - T_2)} = \text{Constant} \quad (16)$$

Condenser of TCES:

The condensation rate of water vapour is estimated as,

$$\dot{Q}_{out,C} = \dot{m}_a \times (h_{in,C} - h_{out,C}) = \dot{m}_{wv,C} \times \Delta H_c \quad (17)$$

where  $\Delta H_c$  (J/kg) represents the latent heat of condensation of water.

When reactors are switched between operating cycles, thermal losses ( $Q_{sl}$ ) can occur. Quantifying these losses as a fraction of the waste heat utilized by the dual reactor system (Reactor 1 + Reactor 2), capturing and upgrading it, can provide valuable insight into its significance in practical operations. The below analysis provides the estimates of switching losses.

$$Q_{sl} = \left[ (mc_p)_{hydrate} + (mc_p)_{reactor} \right] \Delta T \quad (18)$$

Switching losses as a fraction of the total waste heat utilized by Reactor 1 and Reactor 2 is expressed as,

$$\frac{Q_{sl}}{Q_E + Q_{R2}} = \frac{[(mc_p)_{hydrate} + (mc_p)_{reactor}] \Delta T}{m_{wv} (\Delta H_e + c_{p,w} \times (T_1 - T_a) + \Delta H_r^o)} \quad (19)$$

Here,  $c_p$  denotes the specific heat capacity of respective materials. The maximum possible  $\Delta T$  refers to the difference between the hydration temperature and the temperature at which dehydration begins, i.e., the temperature of Reactor 2.

Based on Eq. (19), the thermal mass of reactor should be minimized to reduce thermal losses. At the same time, it must provide a high surface area to ensure efficient heat and mass transfer while accommodating a thin bed of salt hydrate material. For instance, it is reported in the literature that by adopting an embedded cooling tube design, it is possible to design a reactor with a lower thermal mass than that of the active thermochemical energy storage material [33]. As a reference case, when the reactor mass is assumed to be equal to the mass of the salt hydrate, the above equation can be reformulated in terms of heat transfer rates as follows:

$$\frac{\dot{Q}_{sl}}{Q_E + \dot{Q}_{R2}} = \frac{\frac{\dot{m}_{wv}}{wt\%} (c_{p,hydrate} + c_{p,reactor}) \Delta T}{\dot{m}_{wv} (\Delta H_e + c_{p,w} \times (T_1 - T_a) + \Delta H_r^o)} \quad (20)$$

Where, weight percentage (wt%) is defined as a fraction of the mass of water vapour reacted with the salt hydrate material, expressed as,

$$wt\% = \frac{m_{wv}}{m_{hydrate}} = \frac{m_{wv}}{m_{salt} + m_{wv}} \quad (21)$$

#### 4.1. Performance indices

Besides the heat output rate and water vapour loss, system performance is assessed using the following indices that characterize its efficiency.

The efficiency of the TCES is defined as the ratio of the rate of heat upgraded to the rate of heat input into its evaporator and Reactor 2.

$$\text{Efficiency of TCES (\%)} = \frac{\dot{Q}_{R1}}{\dot{Q}_E + \dot{Q}_{R2}} \times 100 \quad (22)$$

The heat upgrade efficiency is defined as the ratio of heat upgraded to the available waste heat from the HTHP.

$$\text{Heat - upgrade efficiency (\%)} = \frac{\dot{Q}_{R1}}{\dot{Q}_{HTP}} \times 100 \quad (23)$$

The overall efficiency is defined as the ratio of the rate of heat utilized by the TCES to the rate of waste heat available from the HTHP.

$$\text{Overall efficiency (\%)} = \frac{\dot{Q}_E + \dot{Q}_{R2}}{\dot{Q}_{HTP}} \times 100 \quad (24)$$

## 5. Results and discussion

This section presents and discusses the results of the thermodynamic analysis of the proposed dual-reactor TCES system for waste heat recovery and upgrading.

Figs. 5(a)-(c) illustrate the overall thermal performance of the system at the evaporator temperature of 100 °C, 95 °C and 90 °C at various waste heat temperatures. For generalizing the concept, the rates of heat exchange (kW<sub>th</sub>) are presented per unit mass flow rate of air (kg/s). The heat input and output both show a pronounced upward trend with rising waste heat temperature ( $T_\theta$ ). The rate of heat upgrade and delivery to the HTHP is governed by the rate of hydration in Reactor 1, which is driven by the rate of water vapour supplied to it. This rate of evaporation, in turn, is dictated by the heat supply to the evaporator, escalating alongside the waste heat temperature. Subsequently, the rate of heat supply to the Reactor 2 also increases. However, the heat input to the TCES system is estimated to increase more significantly as it is quantified as the total thermal energy supplied to both the evaporator and Reactor

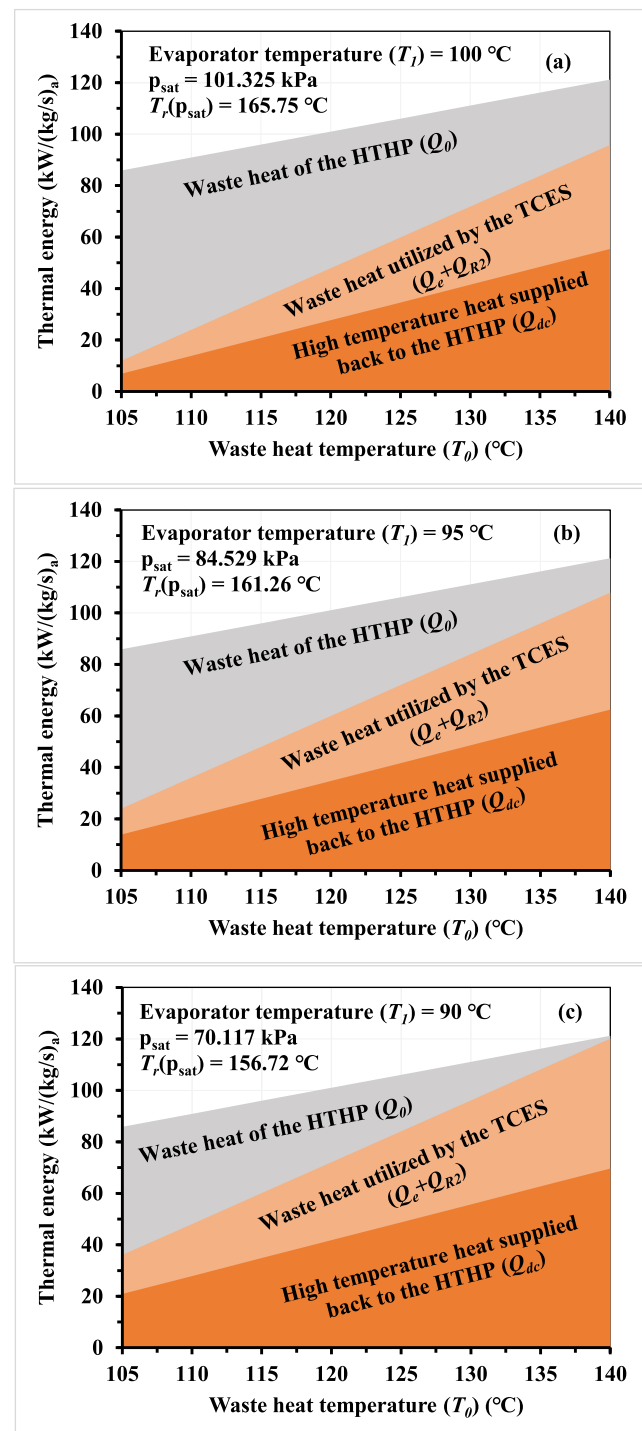


Fig. 5. Thermal performance of the system at the evaporator temperature of (a) 100 °C, (b) 95 °C and (c) 90 °C.

2.

At a waste heat temperature of 105 °C, the total available thermal energy from the HTHP is 85.85 kW/(kg/s)<sub>air</sub>. The heat supplied to the evaporator at this temperature is 5.05, 10.1, and 15.15 kW/(kg/s)<sub>air</sub> when the evaporator operates at 100 °C, 95 °C, and 90 °C, respectively. Correspondingly, the heat transfer rates to Reactor 2 are estimated to be 6.92, 13.88, and 20.89 kW/(kg/s)<sub>air</sub> for these evaporator temperatures. The high-temperature heat returned to the HTHP by Reactor 1 matches the heat input to Reactor 2, as the system is constrained by the requirement for equal water vapour absorption/generation in both

reactors. When the waste heat temperature increases to 140 °C, the heat output from Reactor 1 increases to 55.36, 62.47, and 69.63 kW/(kg/s)<sub>air</sub> at evaporator temperatures of 100 °C, 95 °C, and 90 °C, respectively. This observation from Figs. 5(a)-(c) indicates that, for a given evaporator temperature, higher waste heat temperatures lead to a greater amount of upgraded heat output from Reactor 1 due to an increased supply of water vapour from the evaporator at the required pressure. Conversely, for a fixed waste heat temperature, lowering the evaporator temperature enhances the harnessability of the waste heat. However, the evaporator temperature cannot be reduced indefinitely, as it is constrained by the required heat output temperature of Reactor 1, which depends on the water vapour pressure supplied by the evaporator. Thus, the interplay between the evaporator temperature, waste heat temperature, and reactor requirements dictates the optimal operating conditions for the system. The potential heat loss during the switching between Reactor 1 and Reactor 2 after each cycle, while operating the evaporator in the range of 100 °C to 90 °C and utilizing waste heat at 105 °C to 140 °C is estimated using Eq. (20) to be approximately 10 % of the waste heat utilized by the quasi-continuous thermochemical system integrated into the HTHP process. Here, the values of  $c_p$  for K<sub>2</sub>CO<sub>3</sub> and reactor material (stainless steel 316) are considered as 1.02 k/kgK [34] and 0.5 kJ/kgK, respectively. The energy calculations presented in this study depend on the thermophysical properties of air, water, and the salt hydrate materials used. Consequently, the estimated values may vary slightly based on the accuracy of these properties.

Fig. 6 illustrates the variation in system efficiency across different operating conditions. Notably, the TCES efficiency remains constant at 57.8 % in all cases evaluated. This consistent efficiency is due to the fixed ratio of air temperature change across the evaporator and Reactor 2 (Eq. (16)), which is constrained by the requirement for equal water vapour absorption and desorption in Reactors 1 and 2, respectively. In contrast, both the heat upgrading efficiency and the overall system efficiency show a gradual increase with rising heat source temperature. Specifically, the heat upgrading efficiency rises from 8.1 % to 45.7 %, and the overall efficiency increases from 13.9 % to 79.0 % as the heat source temperature is elevated from 105 °C to 140 °C at an evaporator temperature of 100 °C. At corresponding heat source temperatures, these efficiencies also increase from 16.2 % to 51.5 % and from 27.9 % to 89.1 %, respectively, at an evaporator temperature of 95 °C. At an evaporator temperature of 90 °C, the heat upgrading efficiency increases from 24.3 % to 57.5 %, while the overall efficiency rises from 42.0 % to 99.1 %. These trends highlight the significant impact of heat source temperature on both heat upgrading and overall system performance, with higher efficiencies observed at lower evaporator temperatures.

As mentioned earlier, the condenser is set to 20 °C, and the air, post-

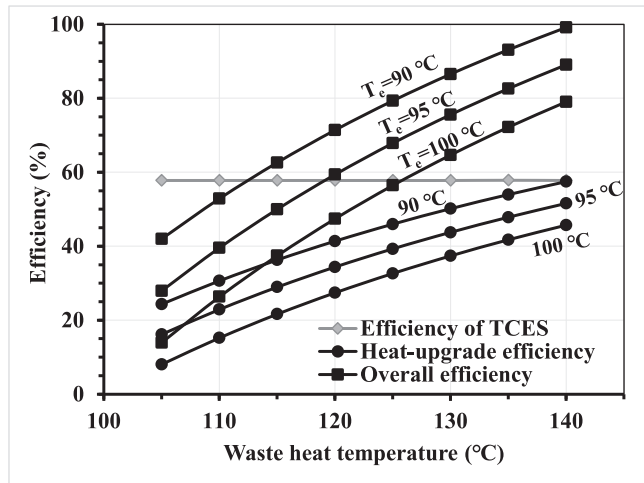


Fig. 6. Efficiency of the system.

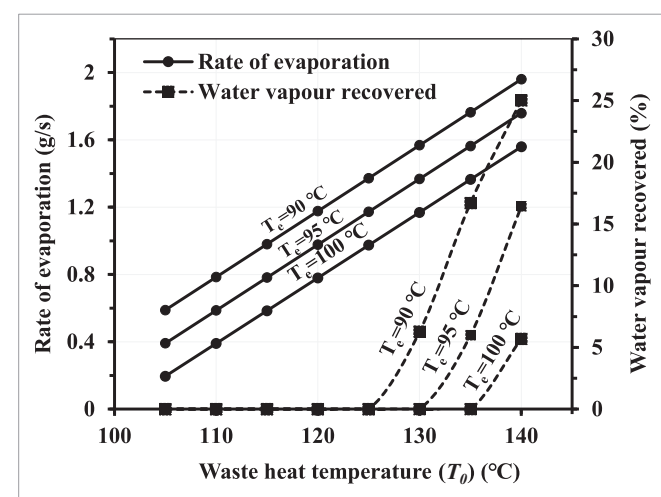


Fig. 7. Recovery of water vapour with condenser at 20 °C.

charging Reactor 2, aims to attain the same temperature at its exit leveraging its maximum utilization for charging. As the temperature of air decreases in the condenser, its saturation pressure decreases and consequently, it loses its ability to hold more water vapour. Thus, it starts condensing till it attains a new equilibrium state with the condenser. The results shown in Fig. 7 indicate that, for a given evaporator temperature ( $T_1$ ) of TCES, the evaporation rate increases with the waste heat temperature ( $T_0$ ) due to the increased heat input. Similarly, at a given waste heat temperature, the vapour pressure of the air exiting Reactor 2 increases as the evaporator temperature of TCES decreases. This is because higher waste heat temperatures result in greater heat transfer, which increases the amount of water vapour participating in the dehydration reaction, leading to more vapour being added to the air stream passing through Reactor 2. Consequently, the potential for improved water vapour recovery in the TCES condenser increases at a given condenser temperature ( $T_a$ ). However, the maximum water vapour recovery is ultimately limited by the condenser temperature. As detailed in Section 2, Fig. 7 illustrates the role of the condenser in the proposed dual-reactor TCES system configuration. The data demonstrates that when the condenser operates at ambient temperature (20 °C), only up to 25 % of the water vapour released by Reactor 2 can be recovered within the operational temperature range. Furthermore, Fig. 7 shows that the minimum waste heat temperature needed for water vapour recovery increases as the evaporator temperature of TCES rises. This is because a higher evaporator temperature reduces the heat transfer rate, which in turn lowers the evaporation rate. As a result, less water vapour releases during the dehydration reaction in Reactor 2, due to the constraint of equal water vapour reaction in Reactors 1 and 2. To increase the amount of water vapour involved in the reaction, higher heat transfer is required. Specifically, at evaporator temperatures of 100 °C, 95 °C, and 90 °C, the corresponding minimum waste heat temperatures required are 135 °C, 130 °C, and 125 °C, respectively. To improve the recovery efficiency of water vapour, the condenser must operate at lower temperatures, which inevitably incurs higher energy costs. These results provide valuable insight into the advantages and limitations of using a condenser at ambient temperature and serve as a basis for determining whether to incorporate the condenser into the system or omit it entirely, depending on the desired trade-offs between recovery efficiency and energy expenditure. It may be noticed that when the ambient temperature is significantly lower, it leads to a higher rate of condensation due to the reduced saturation pressure.

The temperature of the air stream at the outlet of Reactor 2 serves as an indicator of the extent to which the TCES system leverages the waste heat from the HTHP. Fig. 8 illustrates the variation in the air stream temperature exiting Reactor 2 following its charging under different

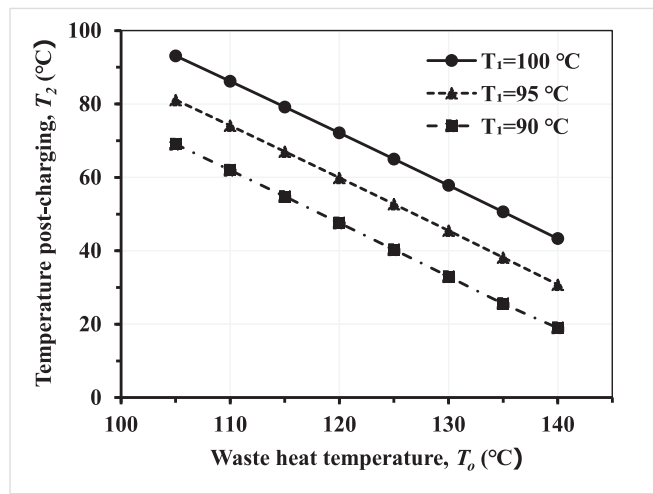


Fig. 8. Air stream temperature at the exit of Reactor 2.

waste heat temperatures at specified TCES evaporator temperatures. The objective is to maximize the thermal energy transfer to Reactor 2, ideally until the HTF temperature approaches the ambient temperature.

From Fig. 8, it is evident that for any given evaporator temperature of the TCES, higher waste heat temperatures result in lower temperatures of air at Reactor 2 exit, indicating enhanced heat utilization during the charging process. This phenomenon can be attributed to the constraint of equal water vapour mass reacted with Reactor 1 and Reactor 2. For instance, at an evaporator temperature of 100 °C, when the waste heat temperature from the HTHP is 105 °C, the small temperature difference ( $\Delta T = 5$  °C) limits the heat transfer to the TCES evaporator. Consequently, the rate of water vapour generation is very low ( $\dot{m} = 0.20$  g/s), subsequently requiring less desorption in Reactor 2, resulting in a minimal reduction in air temperature across the Reactor 2 (7.9 °C). In contrast, when the waste heat temperature is increased to 140 °C, the greater temperature difference ( $\Delta T = 40$  °C) leads to a higher rate of water vapour generation ( $\dot{m} = 1.56$  g/s). As a result, more heat is supplied by air to Reactor 2 to desorb the same amount of water vapour, causing a significant drop in the air stream temperature, amounting to 56.7 °C. A similar rationale holds for cases where the evaporator temperature is 95 °C and 90 °C, with corresponding increases in the waste heat temperature.

Fig. 9 illustrates the variation in specific and relative humidities of

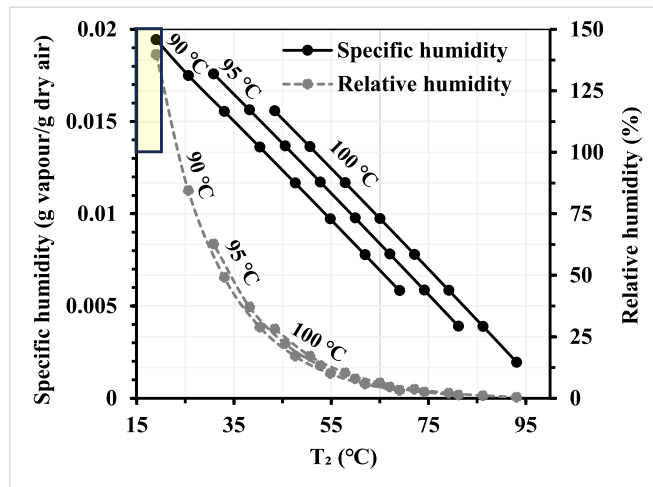


Fig. 9. Specific and relative humidities of air exiting Reactor 2 after charging (dehydration).

the air exiting Reactor 2 after the charging process, plotted as a function of the exit temperature ( $T_2$ ). Lower  $T_2$  values correspond to greater heat transfer to Reactor 2, indicating a higher degree of dehydration within the reactor. This behavior arises from the inherent coupling between heat transfer and gas–solid reactions in salt hydrate systems. At the evaporator temperature of 90 °C and a waste heat source temperature of 140 °C, the calculated relative humidity of 139 % suggests the onset of condensation within Reactor 2. Consequently, operation under these conditions is deemed infeasible. This limitation stems from the imposed operational constraint requiring equal water vapour reaction rates in Reactor 1 and Reactor 2 (Eq. (16)), which ensures consistency in the quasi-continuous operation framework employed in this study.

The present study investigates the thermodynamic performance of the integrated system, considering that Reactor 1 delivers heat to the HTHP evaporator at a temperature close to the reaction temperature of the salt hydrate bed, at the specified supply pressure of water vapour, using heat pipes for efficient heat transfer. However, in practice, the thermal resistance of both the salt hydrate bed and the heat pipes will hinder this ideal scenario. Consequently, the actual heat transfer rates and overall system efficiency will be affected accordingly. Also, the present thermodynamic investigation varies the temperature conditions of the TCES system in one aspect. However, all parameters of both systems are closely interlinked; a change in one parameter can cause continuous changes in all other variables. Therefore, further investigation of the transient performance in the integrated system is needed in this area.

The study poses several challenges for practical implementation, alongside its key advantages. Salt hydrates like  $K_2CO_3$ , which are key to the thermochemical process, can suffer from slow reaction rates, low effective thermal conductivity, and potential deliquescence, all of which may affect long-term stability and efficiency. The switching between the two alternating reactors causes thermal losses, as each reactor must be heated or cooled to the temperature level of the next cycle. It is also essential to ensure that the reacted fraction of salt hydrate beds in both reactors is equal and maximized during these cycles. Additional challenges include efficiently scaling up the system, managing heat transfer, addressing material degradation over time, and ensuring smooth integration with existing infrastructure. However, these challenges may be addressed by modifying the materials to enhance their properties [23,24,35,36], holding promising potential to advance the practical implementation of the concept.

## 6. Conclusion and outlook

The present study discusses the necessity of harnessing waste heat from high temperature mechanical heat pumps and attempts to provide a possible energy-inexpensive solution for heat recovery. It proposes the configuration of a dual-reactor salt hydrate based cascaded heat pump. The waste heat is utilized to generate water vapour for the hydration (discharging) of one reactor and also serves as a driving force for the dehydration (charging) of the other. Special emphasis is placed on the operation of the evaporator, which supplies water vapour to the salt hydrate bed, delivering heat at higher temperatures by leveraging waste heat from the high temperature heat pump. An empirical relation has been developed to determine the required evaporator temperature as a function of the waste heat temperature, the thermal properties of the salt material, and the required heat delivery temperature. Subsequently, a thermodynamic analysis indicates a promising performance of the proposed concept, with heat delivery of 6.9 kW and 55.4 kW per kg/s of air at 105 °C and 140 °C, respectively, with the evaporator of thermochemical system at 100 °C. Based on the analysis presented, the system proposed in this study offers substantial potential for utilizing waste heat, depending on the evaporator temperature, and achieves a thermochemical energy storage efficiency of 57.8 %. The findings highlight the significant impact of the evaporator and condenser on the overall system performance efficiency. The heat upgrade, as well as the overall

performance of the system, are noticed to substantially increase with heat source temperature.

## CRediT authorship contribution statement

**K. Malleswararao:** Writing – original draft, Methodology, Investigation, Formal analysis, Conceptualization. **Inga Bürger:** Writing – review & editing, Supervision, Conceptualization. **Aldo Cosquillo Mejia:** Writing – review & editing, Methodology. **Seon Tae Kim:** Writing – review & editing. **Marc Linder:** Writing – review & editing, Supervision, Project administration.

## Declaration of competing interest

The authors declare that they have no known competing financial interests or personal relationships that could have appeared to influence the work reported in this paper.

## Acknowledgements

The first author would like to express sincere gratitude to the Alexander von Humboldt Foundation for their generous support of this research through the Humboldt Research Fellowships (Ref: 3.5 – IND – 1239729 – HFST-P).

## Data availability

No data was used for the research described in the article.

## References

- [1] Chua KJ, Chou SK, Yang WM. Advances in heat pump systems: a review. *Appl Energy* 2010;87:3611–24. <https://doi.org/10.1016/j.apenergy.2010.06.014>.
- [2] Liu C, Han W, Xue X. Experimental investigation of a high-temperature heat pump for industrial steam production. *Appl Energy* 2022;312:118719. <https://doi.org/10.1016/j.apenergy.2022.118719>.
- [3] Liu C, Jiang Y, Han W, Kang Q. A high-temperature hybrid absorption-compression heat pump for waste heat recovery. *Energ Conver Manage* 2018;172:391–401. <https://doi.org/10.1016/j.enconman.2018.07.027>.
- [4] Marina A, Spoelstra S, Zondag HA, Wemmers AK. An estimation of the European industrial heat pump market potential. *Renew Sustain Energy Rev* 2021;139: 110545. <https://doi.org/10.1016/j.rser.2020.110545>.
- [5] Schmidt M, Linder M. Power generation based on the  $\text{Ca}(\text{OH})_2/\text{CaO}$  thermochemical storage system – experimental investigation of discharge operation modes in lab scale and corresponding conceptual process design. *Appl Energy* 2017;203. <https://doi.org/10.1016/j.apenergy.2017.06.063>.
- [6] M. Richter, E.-M. Habermann, E. Siebecke, M. Linder, A systematic screening of salt hydrates as materials for a thermochemical heat transformer, *Thermochimica Acta*, 659 (2018), pp. 136–150. doi:<https://doi.org/10.1016/j.tca.2017.06.011>.
- [7] Sunku Prasad J, Muthukumar P, Desai F, Basu DN, Rahman MM. A critical review of high-temperature reversible thermochemical energy storage systems. *Appl Energy* 2019;254:113733. <https://doi.org/10.1016/j.apenergy.2019.113733>.
- [8] Malleswararao K, Dutta P, Srinivas Murthy S. Applications of metal hydride based thermal systems: a review. *Appl Therm Eng* 2022;215:118816. <https://doi.org/10.1016/j.applthermaleng.2022.118816>.
- [9] Malleswararao K, Bürger Inga, Mejia Aldo Cosquillo, Kim Seon Tae, Linder Marc. Salt hydrate based thermochemical systems cascaded with high temperature mechanical heat pumps for waste heat recovery. *Energy Conversion and Management*: X 2024;24:100806. <https://doi.org/10.1016/j.ecmx.2024.100806>.
- [10] Richter M, Bouché M, Linder M. Heat transformation based on  $\text{CaCl}_2/\text{H}_2\text{O}$  – part a: closed operation principle. *Appl Therm Eng* 2016;102:615–21. <https://doi.org/10.1016/j.applthermaleng.2016.03.076>.
- [11] Kim ST, Klöppel S, Nicke E, Malleswararao K, Linder M, Stathopoulos P. Assessment of heat storage integration for water vapour compression heat pumps: thermodynamic and techno-economic perspectives. *Int J of Sustain Energy* 2024; 44:2433580. <https://doi.org/10.1080/14786451.2024.2433580>.
- [12] Chen X, Zhang Z, Qi C, Ling X, Peng H. State of the art on the high-temperature thermochemical energy storage systems. *Energ Conver Manage* 2018;177: 792–815. <https://doi.org/10.1016/j.enconman.2018.10.011>.
- [13] Bouché M, Richter M, Linder M. Heat transformation based on  $\text{CaCl}_2/\text{H}_2\text{O}$  – part B: open operation principle. *Appl Therm Eng* 2016;102:641–7. <https://doi.org/10.1016/j.applthermaleng.2016.03.102>.
- [14] Stengler J, Bürger I, Linder M. Thermodynamic and kinetic investigations of the  $\text{SrBr}_2$  hydration and dehydration reactions for thermochemical energy storage and heat transformation. *Appl Energy* 2020;277:115432. <https://doi.org/10.1016/j.apenergy.2020.115432>.
- [15] Michel B, Dufour N, Börtlein C, Zoude C, Prud'homme E, Gremillard L, et al. First experimental characterization of  $\text{CaCl}_2$  coated heat exchanger for thermochemical heat transformer applications in industrial waste heat recovery. *Appl Therm Eng* 2023;227:120400. <https://doi.org/10.1016/j.applthermaleng.2023.120400>.
- [16] Esaki T, Yasuda M, Kobayashi N. Experimental evaluation of the heat output/input and coefficient of performance characteristics of a chemical heat pump in the heat upgrading cycle of  $\text{CaCl}_2$  hydration. *Energ Conver Manage* 2017;150:365–74. <https://doi.org/10.1016/j.enconman.2017.08.013>.
- [17] Papapetrou M, Kosmadakis G, Cipollina A, La Commare U, Micale G. Industrial waste heat: estimation of the technically available resource in the EU per industrial sector, temperature level and country. *Appl Therm Eng* 2018;138:207–16. <https://doi.org/10.1016/j.applthermaleng.2018.04.043>.
- [18] Michel B, Clausse M. Design of thermochemical heat transformer for waste heat recovery: methodology for reactive pairs screening and dynamic aspect consideration. *Energy* 2020;211:118042. <https://doi.org/10.1016/j.energy.2020.118042>.
- [19] Sögiütoglu LC, Donkers PAJ, Fischer HR, Huinink HP, Adan OCG. In-depth investigation of thermochemical performance in a heat battery: cyclic analysis of  $\text{K}_2\text{CO}_3$ ,  $\text{MgCl}_2$  and  $\text{Na}_2\text{S}$ . *Appl Energy* 2018;205:159–73. <https://doi.org/10.1016/j.apenergy.2018.01.083>.
- [20] Gaenin M, Shaik SA, Rindt C. Characterization of potassium carbonate salt hydrate for thermochemical energy storage in buildings. *Energ Buildings* 2019;196: 178–93. <https://doi.org/10.1016/j.enbuild.2019.05.029>.
- [21] Houben J, Sögiütoglu L, Donkers P, Huinink H, Adan O.  $\text{K}_2\text{CO}_3$  in closed heat storage systems, renew. *Energy* 2020;166:35–44. <https://doi.org/10.1016/j.renene.2020.11.119>.
- [22] Donkers PAJ, Sögiütoglu LC, Huinink HP, Fischer HR, Adan OCG. A review of salt hydrates for seasonal heat storage in domestic applications. *Appl Energy* 2017;199: 45–68. <https://doi.org/10.1016/j.apenergy.2017.04.080>.
- [23] Salehzadeh D, Elahi B, ten Elshof JE, Brem G, Mehrali M. Porous potassium carbonate granules with enhanced diffusion kinetics for thermochemical heat storage. *Chem Eng J* 2024;497:154560. <https://doi.org/10.1016/j.cej.2024.154560>.
- [24] Elahi B, Salehzadeh D, de Vos WM, Shahidzadeh N, Brem G, Mehrali M. Boosting stability of  $\text{K}_2\text{CO}_3$  granules for thermochemical heat storage applications through innovative membrane encapsulation. *Chem Eng J* 2024;500:157042. <https://doi.org/10.1016/j.cej.2024.157042>.
- [25] Aydin D, Casey SP, Chen X, Riffat S. Novel “open-sorption pipe” reactor for solar thermal energy storage. *Energ Conver Manage* 2016;121:321–34. <https://doi.org/10.1016/j.enconman.2016.05.045>.
- [26] Michel B, Neveu P, Mazet N. Comparison of closed and open thermochemical processes, for long-term thermal energy storage applications. *Energy* 2014;72: 702–16. <https://doi.org/10.1016/j.energy.2014.05.097>.
- [27] Ng KC, Thu K, Kim Y, Chakraborty A, Amy G. Adsorption desalination: an emerging low cost thermal desalination method. *Desalination* 2013;308:161–79. <https://doi.org/10.1016/j.desal.2012.07.030>.
- [28] Mitra S, Kumar P, Srinivasan K, Dutta P. Performance evaluation of a two-stage silica gel + water adsorption based cooling-cum-desalination system. *Int J Refrig* 2015;58:186–98. <https://doi.org/10.1016/j.ijrefrig.2015.06.018>.
- [29] Thomson GW. The Antoine equation for vapor-pressure data. *Chem Rev* 1946;38: 1–39. <https://doi.org/10.1021/cr60119a001>.
- [30] Lide DR, editor. CRC handbook of chemistry and physics. 85th ed. CRC Press; 2004. p. 6–8 [ISBN 978-0-8493-0485-9].
- [31] Mazur N, Huinink H, Borni B, Sansota S, Fischer H, Adan O. Thermodynamic analysis of dehydration of  $\text{K}_2\text{CO}_3 \cdot 1.5\text{H}_2\text{O}$ . *Thermochim Acta* 2022;715:179286. <https://doi.org/10.1016/j.tca.2022.179286>.
- [32] Cengel YA, Boles MA. *Thermodynamics: An engineering approach*. 6th ed. McGraw-Hill; 2007.
- [33] Raju NN, Muthukumar P, Selvan PV, Malleswararao K. Design methodology and thermal modelling of industrial scale reactor for solid state hydrogen storage. *Int J Hydrogen Energy* 2019;44:20278–92. <https://doi.org/10.1016/j.ijhydene.2019.05.193>.
- [34] Zhao W, Sprachmann G, Li Z, Cai N, Zhang X. Effect of  $\text{K}_2\text{CO}_3 \cdot 1.5\text{H}_2\text{O}$  on the regeneration energy consumption of potassium-based sorbents for  $\text{CO}_2$  capture. *Appl Energy* 2013;112:381–7. <https://doi.org/10.1016/j.apenergy.2013.06.018>.
- [35] Kumar N, Hirshey J, LaClair TJ, Gluesenkamp KR, Graham S. Review of stability and thermal conductivity enhancements for salt hydrates. *J Energy Storage* 2019; 24:100794. <https://doi.org/10.1016/j.est.2019.100794>.
- [36] Mazur N, Huinink H, Fischer H, Adan O. A systematic deliquescent additive selection approach for enhancement of reaction kinetics of thermochemical heat storage materials. *Sol Energy Mater Sol Cells* 2023;263:112588. <https://doi.org/10.1016/j.solmat.2023.112588>.